

Numerical simulation and analysis of dynamic compensation for atmosphere turbulence based on stochastic parallel gradient descent optimization

Huimin Ma (马慧敏), Pengfei Zhang (张鹏飞), Jinghui Zhang (张京会),
Chunhong Qiao (乔春红), and Chengyu Fan (范承玉)*

Key Lab of Atmospheric Composition and Optical Radiation, Anhui Institute of Optics and Fine Mechanics,
Chinese Academy of Sciences, Hefei 230031, China

*Corresponding author: cyfan@aiofm.ac.cn

Received October 24, 2011; accepted February 24, 2012; posted online May 9, 2012

We present the numerical simulation and analysis of the bandwidth estimation for adaptive optics (AO) systems based on stochastic parallel gradient descent (SPGD) optimization. Time-varying atmosphere turbulence due to wind velocity and turbulence structure constant is considered in the dynamic simulation. The performance of SPGD system with different iteration frequencies is studied in detail. A formula given that estimates the Strehl ratio degradation after SPGD adaptive control due to the increasing proportion of the number of deformable mirror actuator times Greenwood frequency to iteration frequency based on numerical analyses, can be used to roughly predict the required iteration frequency under the condition of various Greenwood frequencies.

OCIS codes: 010.0010, 010.1080, 010.1330.

doi: 10.3788/COL201210.S10102.

Recently, adaptive optics (AO) systems based on stochastic parallel gradient descent optimization (SPGD) have shown great potential on compensation of phase distortions induced by wave propagation through atmosphere turbulence^[1,2]. Especially for propagation scenarios in which scintillations become significant and branch-points are present in the received plane, wavefront measurements and reconstruction have nearly failed and compensation performance based on phase conjugation has seriously degraded^[3,4]. The system based on SPGD optimization algorithm is an alter approach for above propagation scenarios, because it does not need wavefront measurement^[5,6]. However, dynamic changes occurring in atmosphere turbulence could impose serious limitations on AO system control bandwidth, because of slow convergence with SPGD technique. This is a challenge issue that dynamic compensation for atmosphere turbulence with SPGD optimization technique.

Temporal dynamics of atmospheric turbulence can be characterized by the parameter f_G , known as Greenwood frequency^[7],

$$f_G = \left[0.102k^2 \int_0^\infty C_n^2(z)v^{5/3}(z)dz \right]^{3/4}. \quad (1)$$

In special case of a uniformity turbulence layer with wind velocity v , the Greenwood frequency may be expressed as

$$f_G = 0.432 \frac{v}{r_0}, \quad (2)$$

where r_0 is the Fried parameter. The value of f_G is determined by the turbulence strength and wind profiles of the atmosphere.

For SPGD compensation system, the time of an iteration period includes response time of the deformable mirror, time for detecting and obtaining performance metric and iteration calculation time. We called this time

period iteration frequency f_s . It is interesting to make an estimation of the SPGD compensation performance degradation based on Strehl ratio with the increase of Greenwood frequency. Analysis of dependences of Strehl ratio degradation and iteration frequency required on Greenwood frequency are examined based on numerical simulations and scaling consideration in this letter.

To investigate the effects of various SPGD iteration frequencies on an AO system for compensation of time-varying atmosphere turbulence, we used a wave-optics code to make some numerical simulations of laser propagating through atmosphere turbulence with an AO system based on SPGD optimization technique. In this letter we consider a laser beam projection system which is designed to generate an AO reference beam provided as a point beacon source located at the target. The schematic of the simulation projection system follows the basic conceptual as shown in Fig. 1. The outgoing beam phase control is based on SPGD optimization of beacon wave, and focused with a transmitting telescope to where the target was located.

The general optical schematic of SPGD compensation system is shown in Fig. 2. This system is composed of a camera that records image plane intensity distribution

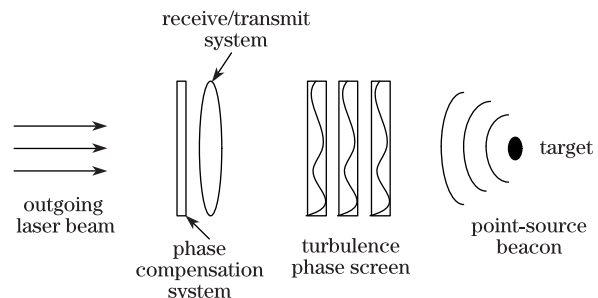


Fig. 1. Schematic of laser projection system.

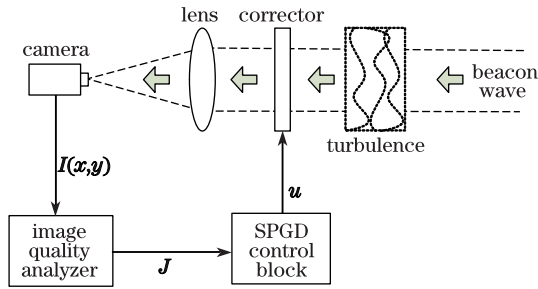


Fig. 2. Schematic of SPGD AO system.

$I(\mathbf{r})$, $\mathbf{r}=(x, y)$, an image quality analyzer that can calculate image quality metric $J = J(\mathbf{u})$, and a control block SPGD algorithm that produces control signals \mathbf{u} for a deformable mirror. The phase introduced by deformable mirror is^[8]

$$\psi(x, y) = \sum_{j=1}^N u_j S_j(x, y), \quad (3)$$

where u_j represents the j th actuator amplitudes, and N is the actuator number of deformable mirror. Since the experimental results show that the Gaussian represents a deformable mirror influence function quite well^[8], the expression of the influence function $S_j(x, y)$ is described as

$$S_j(x, y) = \exp\left(\ln p \frac{(x - x_j)^2 + (y - y_j)^2}{r_d^2}\right), \quad (4)$$

where (x_j, y_j) denotes the location coordinates of the j th actuator, p represents the coupling factor between the adjacent actuators, and r_d is the distance between the adjacent actuators.

In the simulation, we define mean radius in the focal plane as the image quality metric J , and the calculation formula is

$$J = \frac{\iint_D \sqrt{(x - x_0)^2 + (y - y_0)^2} I(x, y) dx dy}{\iint_D I(x, y) dx dy}, \quad (5)$$

where D is the area occupied by laser intensity distribution, (x_0, y_0) is the centroid coordinates of image and $I(x, y)$ is the far field light intensity in position (x, y) . Stochastic parallel perturbation technique requires small random perturbation $\delta u^{(n)} = \{\delta u_1, \delta u_2, \dots, \delta u_j, \dots, \delta u_N\}^{(n)}$. The perturbation δu_j is a random number which has fixed amplitude $|\delta u_j| = \sigma$ and equal probabilities for $\delta u_j = \sigma$ and $\delta u_j = -\sigma$ ^[9,10]. The performance metric change δJ caused by the control perturbation δu_j can be measured. $\delta J^{(n)} \delta u^{(n)}$ is used as the gradient estimate components, so the control signals are updated with the rule

$$u^{(n+1)} = u^{(n)} + \gamma \delta J^{(n)} \delta u^{(n)}, \quad (6)$$

where n is the iteration number and γ is the gain coefficient. In the application, $\delta J^{(n)}$ is achieved by measurement and calculated as

$$\delta J^{(n)} = J(u^{(n)} + \delta u^{(n)}) - J(u^{(n)} - \delta u^{(n)}). \quad (7)$$

For the sake of simplicity, the wind velocity v and turbulence structure constant C_n^2 are considered to be constant in the propagation path. In the simulation, the performance of SPGD system was tested in the case of SPGD iteration frequencies of 1, 10, and 100 kHz for various dynamic turbulence scenarios. We fixed the propagation length of 10 km, and set r_0 as 0.2, 0.12, 0.086 m through changing the turbulence structure constant C_n^2 . For every r_0 and every iteration frequency situation, we implemented the simulation under the condition of wind velocities $v=0.0, 1.0, 4.0, 8.0, 12.0, 16.0$ m/s. The main parameters used in the simulation are presented in Table 1.

Table 1. Parameters Used in the Simulation

Parameter	Value
Receive or Transmit Aperture Diameter, D (cm)	60
Wavelength, $\lambda_{\text{main}} = \lambda_{\text{beacon}}$ (μm)	1.06
Propagation Length, L (km)	10
Turbulence Structure Constant, C_n^2 ($\text{m}^{-2/3}$)	$3.0 \times 10^{-16} / 7.02 \times 10^{-16} / 1.23 \times 10^{-15}$
Grid Number, N_g	256×256
Grid Sampling Interval, Δx (cm)	1
Number of Phase Screen, N_{ps}	20
Number of Deformable Mirror Actuator, N	61
Distance of Adjacent Actuators r_d (cm)	7.5
Actuators Coupling Factor p	15%
Distribution Amplitude $ \delta u $	0.5
Gain Coefficient γ	Adaptive Coefficient

The performance results are given for various simulation situations. In all cases, the peak Strehl ratio in the plane where the target located was given. The results are averaged on 50 atmosphere realizations for each case tested. First, we consider SPGD system with a clock frequency of 1 000 iterations/sec specially. The average Strehl ratio evolution curves with expect to different wind velocities for the turbulence distortion $r_0 = 0.12$ m are shown in Fig. 3(a). It states that the system performance degrades as wind velocity increases, and it nearly loses correction ability when $v > 8$ m/s. The average Strehl ratio evolution curves with expect to different values of r_0 for the wind velocities $v = 1$ m/s are shown in Fig. 3(b). We can see that the system performance also degrades as the value of r_0 decreases. From the curves, it reveals that the Strehl ratio always can be improved in the beginning, but in the following the iteration process fails to find the extrema of performance metric and is trapped by the local extrema due to time-varying turbulence induced by nonzero wind velocity. According to Eq. (2), Greenwood frequency increases as wind velocity v increases or Fried parameter r_0 decreases. Then we can deduce that the system performance degrades as Greenwood frequency increases, because the iteration frequency of 1 kHz does not satisfied the situations.

To examine degradation of the Strehl ratio only due to the iteration frequency, we studied Strehl ratio value

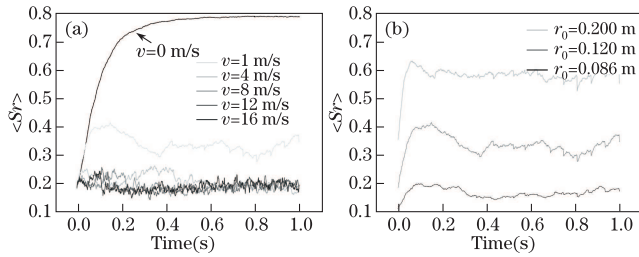


Fig. 3. Evolution curves of $\langle Sr \rangle$ with respect to the condition of (a) different wind velocities, $r_0 = 0.12\text{ m}$ and (b) different Fried parameters r_0 , $v = 1\text{ m/s}$.

normalized by that in the case of zero wind velocity. The evolution curves of the value of $\frac{\langle Sr \rangle}{\langle Sr_{v=0} \rangle}$ for various r_0 and iteration frequency f_s are shown in Fig. 4. The value of $\frac{\langle Sr \rangle}{\langle Sr_{v=0} \rangle}$ always gets convergence as the close-loop time increases, and tends to a stable level. The Strehl ratio degrades with the increase of wind velocity, but the convergence rate and the final stable value increases as iteration frequency f_s increases. The black curve in each figure represents average convergence curve for every instability evolution curve.

According to the results shown in Fig. 4, we obtained the saturation value for each evolution curve from each corresponding red curve. Figure 5 shows the saturation value of $\frac{\langle Sr \rangle}{\langle Sr_{v=0} \rangle}$ versus Nf_G/f_s , where N is the number of deformable mirror actuators. We processed curve-fitting for these points with the following procedure:

$$\frac{\langle Sr \rangle}{\langle Sr_{v=0} \rangle} = 1 - B \times \exp\left(-A\left(\frac{Nf_G}{f_s}\right)^{-5/3}\right). \quad (8)$$

The fitting-curves denoted by the black curves are presented in Fig. 5. It reveals that for a certain value of r_0 , the Strehl ratio decrease with the form of Eq. (8) as the ratio of the Greenwood frequency f_G to the SPGD iteration frequency f_s increases. The times value of the iteration frequency f_s to Greenwood frequency Nf_G are given in Table 2 under the conditions of $\langle Sr \rangle$ up to 70% and 90% of the value of $\langle Sr_{v=0} \rangle$ for various value of r_0 . It is estimated that for SPGD system the required iteration frequency is approximately from 10 to 40 times Nf_G , which accords with the results in Ref. [11] in which the deformable mirror with 21 actuators using 1, -2, -4 kHz iteration frequencies was tested. However, it is still concluded that the iteration frequency required increasing to keep better value of $\frac{\langle Sr \rangle}{\langle Sr_{v=0} \rangle}$ as the value of r_0 decreases from the simulation results.

Table 2. Value of $\frac{f_s}{Nf_G}$ for Different r_0

r_0/m	$\frac{f_s}{Nf_G}$ (70%)	$\frac{f_s}{Nf_G}$ (90%)
0.20	6.6326	12.1577
0.12	11.8550	18.6017
0.086	24.3276	37.6374

In conclusions, we present some dynamic compensation results for atmosphere turbulent based on SPGD optimization. The time-varying distortions are always compensated by SPGD system to different degrees. However, SPGD adaptive system requires very high iteration frequency in the presence of a dynamic optical turbulence, especially with high Greenwood frequency. A formula

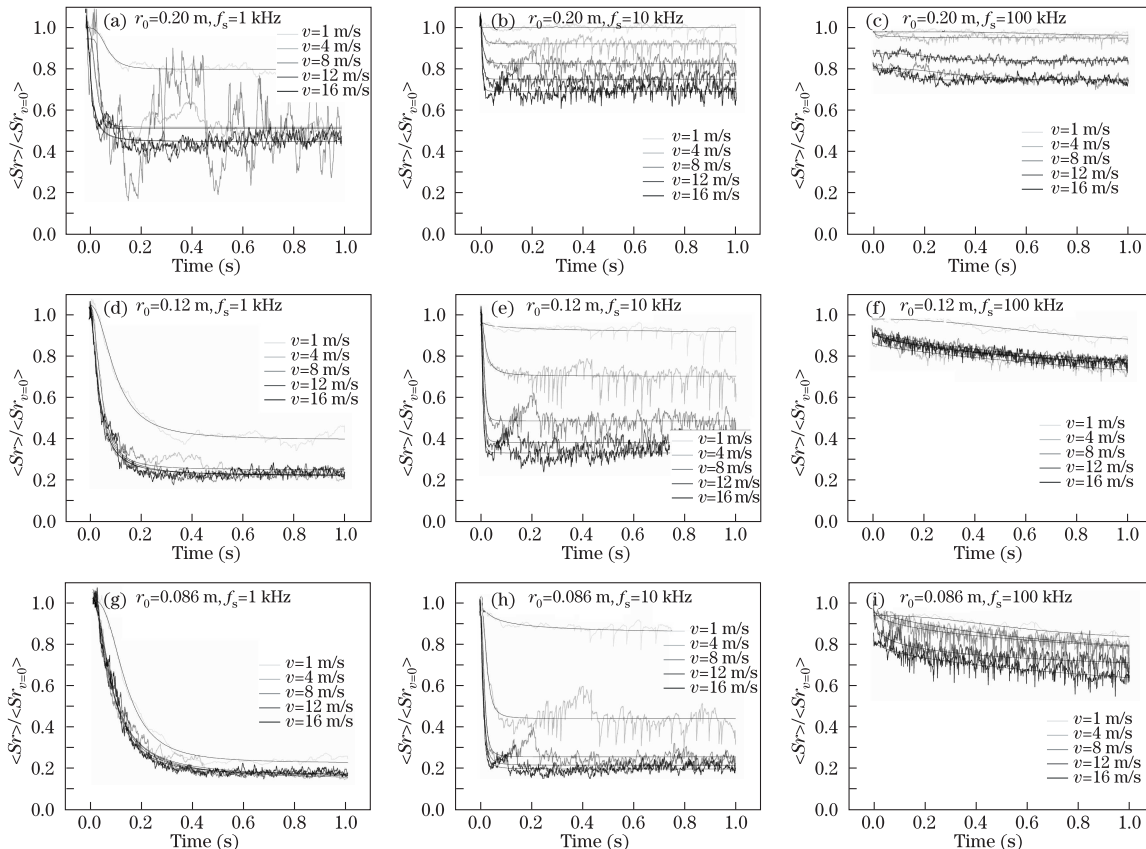


Fig. 4. (Color online) Evolution curves for various r_0 , wind velocity, and iteration frequency f_s .

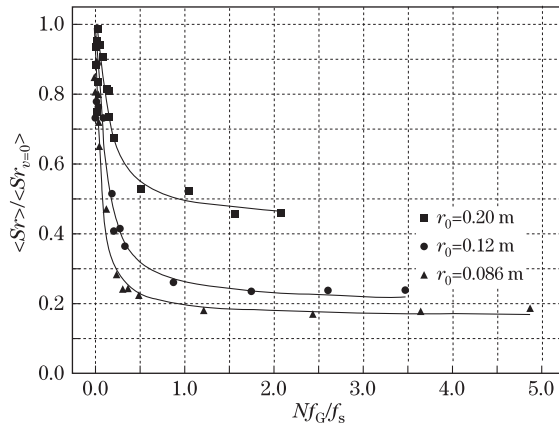


Fig. 5. Saturation value of $\langle Sr \rangle / \langle Sr_{v=0} \rangle$ versus Nf_G / f_s , and the fitting-curves.

that estimates the Strehl ratio degradation after adaptive control due to the value of Nf_G / f_s increasing based on numerical analyses, which can be used to predict the performance of the SPGD control systems and the required iteration frequency under the condition of various Greenwood frequencies. The iteration frequency required increases with the decrement of r_0 and with the increment of a factor Nf_G with Greenwood frequency and actuator number of wavefront corrector. Hence, future work must examine ways to reduce the required iteration

frequency of this system. The results may have some theoretical significance for practical system.

References

1. T. Weyrauch and M. A. Vorontsov, *Appl. Opt.* **44**, 6388 (2005).
2. T. Weyrauch and M. A. Vorontsov, *Proc. SPIE* **5162**, 1 (2003).
3. N. B. Baranova, A. V. Mamaev, N. F. Pilipetsky, *J. Opt. Soc. Am. A* **73**, 525 (1983).
4. C. A. Primmerman, T. R. Price, R. A. Humphreys, B. G. Zollars, H. T. Brarclay, J. Herrmann, *Appl. Opt.* **34**, 2081 (1995).
5. M. A. Vorontsov and G. W. Carhart, *Opt. Lett.* **22**, 907 (1997).
6. M. A. Vorontsov and G. W. Carhart, *J. Opt. Soc. Am. A* **17**, 1440 (2000).
7. F. Roddier, *Adaptive Optics in Astronomy* (Cambridge University, Cambridge, 1999).
8. R. K. Tyson, *Principle of Adaptive Optics* (Academic Press, Carolina 1991).
9. J. C. Spall, *IEEE Trans. Autom. Control.* **37**, 332 (1992).
10. J. C. Spall, *Introduction to Stochastic Search and Optimization* (Wiley, Hoboken, 2003).
11. A. J. Masino and D. J. Link, *Proc. SPIE* **58950T**, 1 (2005).